Bioelectrochemistry 96 (2014) 37–42

Contents lists available at ScienceDirect

Bioelectrochemistry

journal homepage: www.elsevier.com/locate/bioelechem

Amperometric glucose biosensor based on layer-by-layer films of microperoxidase-11 and liposome-encapsulated glucose oxidase

J.S. Graça [a], R.F. de Oliveira [b], M.L. de Moraes [c], M. Ferreira [a,*]

[a] Federal University of São Carlos, UFSCar, Campus Sorocaba, 18052-780 Sorocaba, SP, Brazil
[b] São Paulo State University, UNESP, Postgraduate Program in Materials Science and Technology, 17033-360 Bauru, SP, Brazil
[c] Federal University of São Paulo, UNIFESP, Campus São José dos Campos, 12231-280 São José dos Campos, SP, Brazil

ARTICLE INFO

Article history:
Received 23 September 2013
Received in revised form 27 December 2013
Accepted 4 January 2014
Available online 17 January 2014

Keywords:
Glucose biosensor
Microperoxidase-11
Layer-by-layer technique
Liposome
Biosensor

ABSTRACT

An important step in several bioanalytical applications is the immobilization of biomolecules. Accordingly, this procedure must be carefully chosen to preserve their biological structure and fully explore their properties. For this purpose, we combined the versatility of the layer-by-layer (LbL) method for the immobilization of biomolecules with the protective behavior of liposome-encapsulated systems to fabricate a novel amperometric glucose biosensor. To obtain the biosensing unit, an LbL film of the H_2O_2 catalyst polypeptide microperoxidase-11 (MP-11) was assembled onto an indium-tin oxide (ITO) electrode followed by the deposition of a liposome-encapsulated glucose oxidase (GOx) layer. The biosensor response toward glucose detection showed a sensitivity of 0.91 ± 0.09 (μA/cm^2)/mM and a limit of detection (LOD) of 8.6 ± 1.1 μM, demonstrating an improved performance compared to similar biosensors with a single phospholipid-liposome or even containing a non-encapsulated GOx layer. Finally, glucose detection was also performed in a zero-lactose milk sample to demonstrate the potential of the biosensor for food analysis.

1. Introduction

Preserving the activity of immobilized enzymes is a crucial factor for developing successful biosensors based on enzyme catalysis [1–3]. Thus, several strategies, such as physical adsorption, covalent binding, entrapment and cross-linking, have been explored to retain the enzyme native structure onto various types of electrodes [4–6]. These immobilization protocols may affect biosensor efficiency in terms of operational and storage stabilities, sensitivity, selectivity, response time and reproducibility [7], which is related to the enzyme orientation, loading, mobility, stability, structure and biological activity during and after immobilization. For this reason, intensive efforts have been made to employ a successful immobilization strategy that ensures an improved biosensor performance [2]. The layer-by-layer technique (LbL), a widely explored adsorption method, has been an effective approach for enzyme immobilization due to its simplicity and the mild conditions during the film formation [8,9]. Because most enzymes are water-soluble and charged in solution, the LbL method is suitable for assembling different enzyme architectures with low denaturing effects [10,11]. The LbL method can be basically described as a deposition procedure for immobilization of oppositely charged species such as polymers, proteins and nanoparticles, from aqueous solutions [11]. Although many different forces may be involved in film formation, most LbL assemblies are driven by electrostatics [11]. Due to its unique characteristics, such as its applicability to a wide variety of materials, low-cost and biocompatibility, the LbL method has been extensively used in many applications. These include light-emitting diodes (LEDs) [12], solar cells [13], and field-effect transistors [14] as antibacterial [14] and antireflective [15] coatings and many other applications [16].

In biosensing, LbL films have been used in various ways. Ferreira et al., for example, reported a successful strategy for glucose detection using LbL films of glucose oxidase (GOx) and polyallylamine hydrochloride (PAH) on modified electrodes [17]. Lee et al. developed a label-free immunoassay method using an LbL network of carbon nanotubes for detecting swine influenza H1N1virus [18]. Xiang et al. assembled multi-enzyme LbL films of carbon nanotubes for the electrochemical monitoring of important cancer biomarkers [19]. An overview of LbL applications in biosensing and related fields has recently been published [11]. In addition to the LbL strategy, liposome encapsulation has been exploited to preserve the native structure of biomolecules for biosensing [20,21]. The enclosed structure of a liposome shell isolates the encapsulated biomolecule from possible environmental stresses caused by unsuitable pH, ionic strength and temperature [20,21]. Yoshimoto et al., for instance, obtained higher storage and thermal stabilities for yeast alcohol dehydrogenase encapsulated in liposomes [22]. Petri et al. used LbL films to achieve an improved biosensor response when HIV p17-1 peptide was protected by liposomes [20]. The secondary

* Corresponding author at: UFSCar, Rodovia João Leme dos Santos, Km 110 - SP - 264, Bairro do Itinga, Sorocaba, SP, Brazil. Tel.: +55 15 3229 5969.
E-mail addresses: ju_graca@yahoo.com.br (J.S. Graça), furlanrafa@hotmail.com.br (R.F. de Oliveira), marli.moraes@gmail.com (M.L. de Moraes), marystela@ufscar.br (M. Ferreira).

1567-5394/$ – see front matter © 2014 Elsevier B.V. All rights reserved.
http://dx.doi.org/10.1016/j.bioelechem.2014.01.001

structure of the peptide incorporated into liposomes was preserved, but the same did not apply to LbL films with unprotected p17-1. Liu et al. [23] recently reviewed the use of liposomes in biosensors.

In this work, the benefits of liposome encapsulation for preserving the native structure of proteins were investigated in the response of LbL-based glucose biosensors. We exploited the H_2O_2 catalytic properties of microperoxidase-11 (MP-11) as an electron mediator element. MP-11 was chosen due to its relatively simple structure and the similarity of its catalytic behavior to that of peroxidase enzymes. Single phospholipid-liposomes and a mixture of two phospholipids were tested for GOx encapsulation. The biosensor containing MP-11 and a liposome-encapsulated GOx layer was used to detect glucose in zero-lactose samples to demonstrate its potential in food analysis.

2. Experimental details

2.1. Materials

The microperoxidase-11(MP-11),disodium salt from equine heart cytochrome c, 1925 g/mol, with an isoelectric point at pH 4.75 [24] and optimal activity between pH 4.5 and 8.0 [24] was purchased from Sigma Aldrich. Glucose oxidase (GOx) from *Aspergillius niger* (E.C. 1.1.3.4), 118 units/mg, with an isoelectric point at pH 4.2 [25], pKa of 8.2 [25] and optimal activity between pH 3.5 and 6.5 [25], was purchased from Fluka. Poly(ethylene imine) (PEI) and the phospholipids 1-palmitoyl-2-oleoyl-sn-glycero-3-phosphoglycerol(POPG) and 1,2-dipalmitoyl-phosphatidylglycerol (DPPG) were purchased from Sigma-Aldrich and Avanti Polar Lipids, respectively. Glucose (Sigma-Aldrich) solutions used to determine the biosensor response were allowed to mutarotate overnight. All other reagents were of analytical grade and used without further purification.

2.2. Methods and instrumentation

The LbL films were assembled onto quartz and ITO-coated glass substrates (indium-tin oxide, one side coated on glass by Delta Technologies) for spectroscopic and electrochemical measurements, respectively. The quartz substrates were previously cleaned in $HCl/H_2O_2/H_2O$ (1:1:6) (v/v) and $NH_4OH/H_2O_2/H_2O$ (1:1:5) (v/v) solutions, both for 10 min at 80 °C. ITO substrates were cleaned using chloroform, isopropanol and ultrapure water (Milli-Q).

Solutions of MP-11 (0.15 mg/mL), PEI (1 mg/mL), GOx and liposome-encapsulated GOx (both 1 mg/mL) were all prepared in phosphate buffer solution (PBS) at 10 mM and pH 6.3. For spectroscopic measurements, a 2-bilayer precursor LbL film of PEI/PVS (polyvinylsulfonic acid) was assembled onto quartz to reduce the influence of the substrate morphology on film growth [20]. Afterwards, 8-bilayer LbL films were produced by alternately dipping the substrate into the polycationic solution (PEI) for 3 min and the anionic solution (MP-11) or liposome-encapsulated GOx for 10 or 5 min, respectively, with a rinse step in PBS for 30 s in between. The multilayer buildup was monitored at each deposition step using a Genesys 6 UV–visible spectrophotometer (Thermo Fischer). The growth curves were plotted using the average values of absorbance obtained from three different experiments. The solutions of liposome-encapsulated GOx were prepared as described elsewhere [26]. Here, GOx was encapsulated into a mixture of DPPG + POPG (1:4) (v/v) liposomes. This ratio was chosen after an optimization study (results not shown). A single bilayer of GOx or (GOx + POPG + DPPG) was assembled on a 2-bilayer PEI/MP-11 film on ITO to produce two biosensing units. For this purpose we employed deposition times of 3 min in PEI solution, and 30 min in GOx or liposome-encapsulated GOx solutions.

Circular dichroism (CD) spectroscopy was used to analyze the GOx structure in solution (both free and incorporated into the liposome mixture) and also as an LbL film. CD spectra in PBS were collected using a quartz cell of 1 mm optical path. The CD spectra of the 10-bilayer PEI/GOx and PEI/liposome-encapsulated GOx LbL films were performed on quartz substrates. In this case, the optical path was given by the film thickness. Measurements were performed on a J-815 CD spectrometer (Jasco Inc.), with a band width of 1 nm, a response time of 0.5 s and a scanning speed of 100 nm/min. CD spectra were obtained by averaging eight scans.

Amperometric measurements were carried out in a 3-electrode electrochemical cell (7 mL) at room temperature using an Autolab PGSTAT 30 (Echochemie). A platinum sheet (1 cm^2) was used as the counter electrode and the LbL-modified ITO substrates were used as the working electrodes. All potentials were referred to a saturated calomel electrode (SCE). All electrochemical data were acquired in PBS (10 mM, pH 6.3) under stirring and at 50 mV [27]. Glucose and H_2O_2 solutions were also prepared in PBS for determining the biosensor response and MP-11 activity, respectively. All amperometric experiments were performed three times, and the sensitivity and limit of detection (LOD) values were obtained as an average. Before all amperometric experiments the potential of each biosensor was held at the operating value, allowing the background current to decay to a steady-state value.

3. Results and discussion

Scheme 1 shows the idealized structure of the glucose biosensor. A 2-bilayer LbL film of PEI/MP-11 was assembled onto the ITO electrode, followed by the deposition of a single bilayer of PEI/liposome-encapsulated GOx.

The detection mechanism relies on the cascade reaction shown by Eqs. (1) to (4). The initial catalysis of β-D-glucose by GOx produces H_2O_2, which is subjected to MP-11 catalysis and produce the electrical signal [28].

$$\beta\text{-D Glucose} + O_2 \xrightarrow{GOx} \text{Gluconic acid} + H_2O_2 \quad (1)$$

$$\text{MP-Fe}^{+3} + H_2O_2 \leftrightarrow \left[\text{MP-Fe}^{+3}/H_2O_2\right] \rightarrow \text{MP}_{Ox1} + H_2O \quad (2)$$

$$\text{MP}_{Ox1} + e^- + H^+ \rightarrow \text{MP}_{Ox2} \quad (3)$$

$$\text{MP}_{Ox2} + e^- + H^+ \rightarrow \text{MP-Fe}^{+3} + H_2O \text{ at the electrode} \quad (4)$$

where MP_{Ox1} and MP_{Ox2} are two intermediate forms of MP-11[29].

3.1. PEI/MP-11 LbL film growth and activity

Fig. 1 shows the UV–vis absorption spectra for the 8-bilayer PEI/MP-11 LbL film. The absorbance increase at 413 nm was monitored for each deposited layer (inset in Fig. 1). The pronounced band at approximately 413 nm in the film spectra can be assigned as the Soret band, which is assigned to the π → π* transition in the porphyrin cycle of the heme group of MP-11 [30,31]. Less intense bands at ca. 354 and 530 nm can be attributed to the N and Q bands, respectively [30,31]. The Soret band in Fig. 1 is red shifted, from 400 to 413 nm, compared to the MP-11 solution spectrum (not shown). This shift is consistent with a more non-planar conformation of the porphyrin macrocycle [32]. Astuti et al. observed a red shift of the Soret band from 400 to 409 nm when MP-11 was removed from PBS and immobilized onto a SnO_2 electrode using the polycationic binder poly-L-lysine [33]. Huang et al. observed a 10 nm red shift when MP-11 was immobilized in cationic lipid vesicles, but no band shift occurred when neutral lipids were used [32]. A subsidiary experiment (not shown) was performed by titrating PEI droplets into the MP-11 solution, in a manner similar to that reported by Astuti et al. using also PEI and DDAB (dodecyldimethylammonium bromide) solutions [33]. In both cases, an 8 to 10 nm red shift was observed. All of these results are consistent with a slight change in the MP-11 microenvironment due to the presence of cationic species, similar to the PEI/MP-11 LbL films reported here. This film also shows a

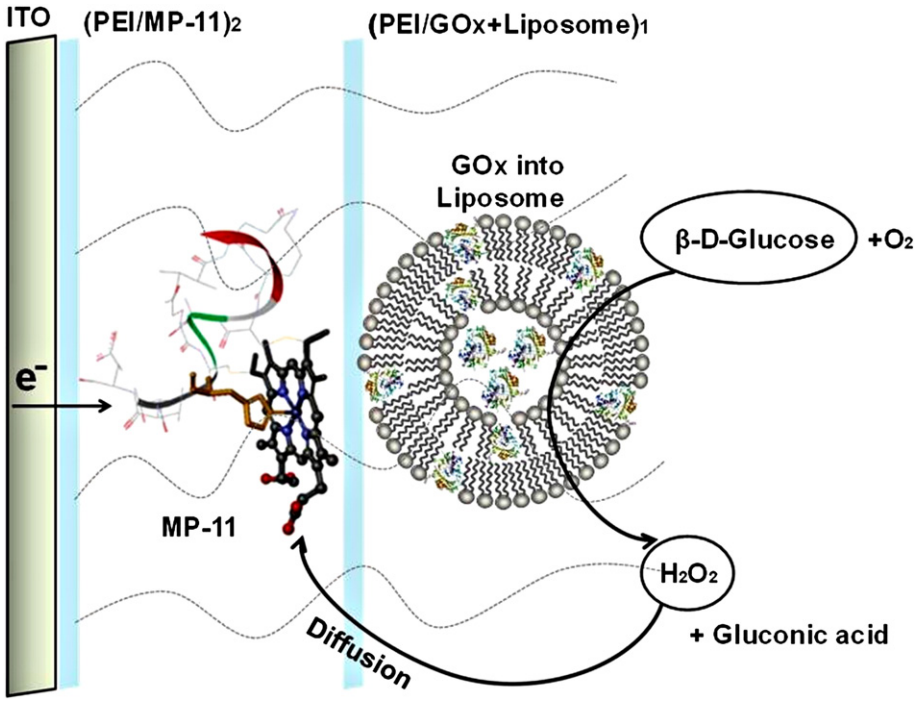

Scheme 1. Idealized biosensor structure and the detection mechanism involved.

growth regime with some saturation trend above 8 bilayers (inset in Fig. 2).

The PEI/MP-11 film activity and sensitivity toward H_2O_2 catalysis are shown in Fig. 2. The amperometric response of a 2-bilayer PEI/MP-11 film onto ITO was recorded for successive additions of 90 μL of H_2O_2. Aliquots of H_2O_2 produced a reasonable increase in current due to the H_2O_2 catalysis by MP-11 and further electron transfer with ITO. Each addition in Fig. 2 corresponds to an increase of 0.025 mM in the H_2O_2 concentration. The inset shows a sensitivity of 2.14 ± 0.10 (μA/cm^2)/mM for the PEI/MP-11 film with a LOD of approximately 5.7 ± 1.4 μM (signal-to-noise ratio of 3). We have also tried to detect glucose with cyclic voltammetry (results not shown) but the redox peaks were not well defined.

To the best of our knowledge there are only two reports on LbL assembly of MP-11 [34,35]. Xu et al. investigated the electrocatalytic properties of chitosan/multi-walled carbon nanotube/MP-11 LbL films [34], and Cipriano et al. fabricated H_2O_2 biosensors using LbL multilayers of PAH and MP-11-modified peptide nanotubes [35]. However, none of these reports have exploited MP-11 LbL films as electron mediators for cascade reactions in glucose biosensors.

3.2. Structural analysis of the GOx in solution and as LbL film

Fig. 3 shows the CD spectra of free and encapsulated GOx in solution (dashed lines) and in LbL films (solid lines). The spectra for free and encapsulated GOx in PBS exhibited two minima at 208 and 219 nm, which are characteristic of an α-helical conformation. For PEI/GOx adsorbed onto a solid substrate, the random coil conformation was clearly formed with a minimum at approximately 221 nm. However, the interaction between GOx and PEI on a solid surface causes some protein denaturing. The CD spectra for liposome-encapsulated GOx in solution and immobilized with PEI showed two minima at 210 and 220 nm. Although the minima were less intense than those for GOx in solution, the CD spectrum indicates the preservation of the helix structure. This result corroborates the data reported by Petri et al. for LbL films containing the p17-1 peptide protected by DPPG liposomes. The secondary

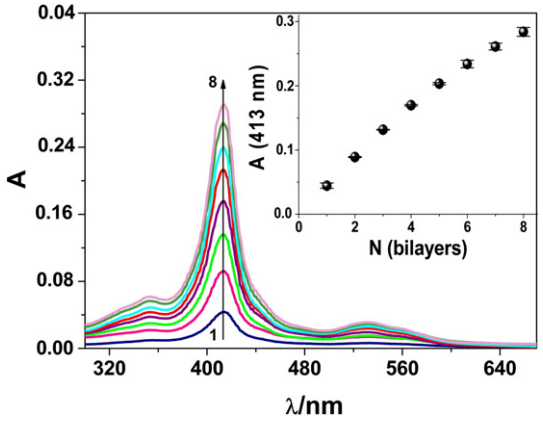

Fig. 1. UV–vis spectra of PEI/MP-11 film. Inset: absorbance versus number of bilayers at 413 nm.

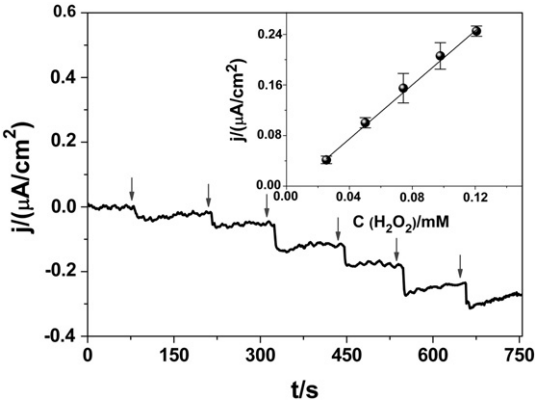

Fig. 2. (PEI/MP-11)$_2$ response to H_2O_2 in PBS (10 mM, pH 6.3) at 50 mV (vs SCE). Additions correspond to an increase of 0.025 M in H_2O_2 concentration. Inset: linear range analytical curve.

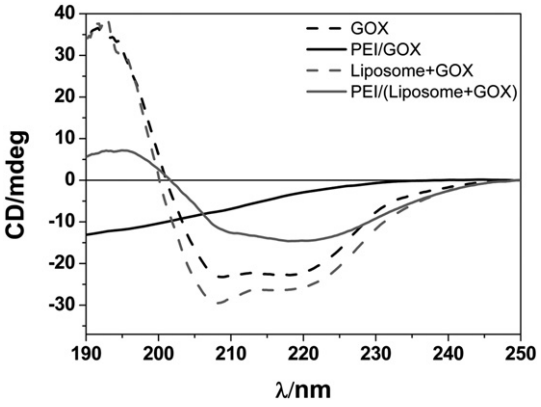

Fig. 3. Circular dichroism spectra for free and liposome-encapsulated GOx in solution and as LbL film.

structure of the peptide incorporated into liposomes was preserved, but the same did not apply to the LbL films with unprotected p17-1. Here, spectra deconvoluted using the Selcon and Contin methods revealed a structure predominantly consisting of helical elements (approximately 82% and 90%, respectively) for the free and liposome-encapsulated GOx. The PEI/GOx film showed 33% of helical elements, 15% of turns and 52% of disordered elements while in the PEI/liposome-encapsulated GOx film 60% of helical elements, 9% of turns and 31% of disordered forms were found. These results agree with the electrochemical data to be presented later on, in which greater sensitivity and stability were obtained for films containing GOx immobilized into liposomes.

3.3. Fabrication of glucose biosensors

We explored the LbL assembly of liposome-encapsulated GOx using a 1:4 (v/v) mixture of two lipids. Prior to biosensor fabrication, GOx was encapsulated into a POPG + DPPG liposome and assembled together with PEI onto quartz substrates. Fig. 4 shows the UV–vis absorption spectra of each bilayer of an 8-bilayer PEI/liposome-encapsulated GOx film. The broad absorption band at 280 nm can be assigned as the absorption of aromatic amino acids residues (mostly tryptophan) of GOx [25]. The inset in Fig. 4 shows a nearly linear increase in absorbance for each layer, suggesting successful deposition of encapsulated GOx using the POPG and DPPG mixture.

For the biosensing unit, a 2-bilayer PEI/MP-11 LbL film was assembled onto ITO, followed by deposition of a single-layer film of PEI/(GOx + POPG + DPPG). Fig. 5A shows the amperometric response of the $(PEI/MP\text{-}11)_2/PEI/(GOx + POPG + DPPG)_1$ biosensor. Its performance was also compared with that of the non-encapsulated GOx

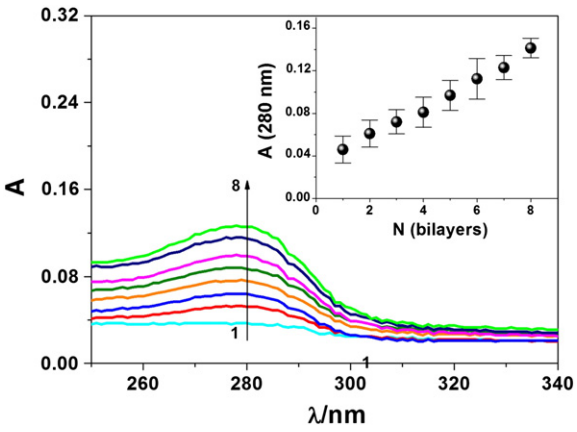

Fig. 4. UV–vis spectra of PEI/liposome-encapsulate GOx film. Inset: absorbance versus number of bilayers at 280 nm.

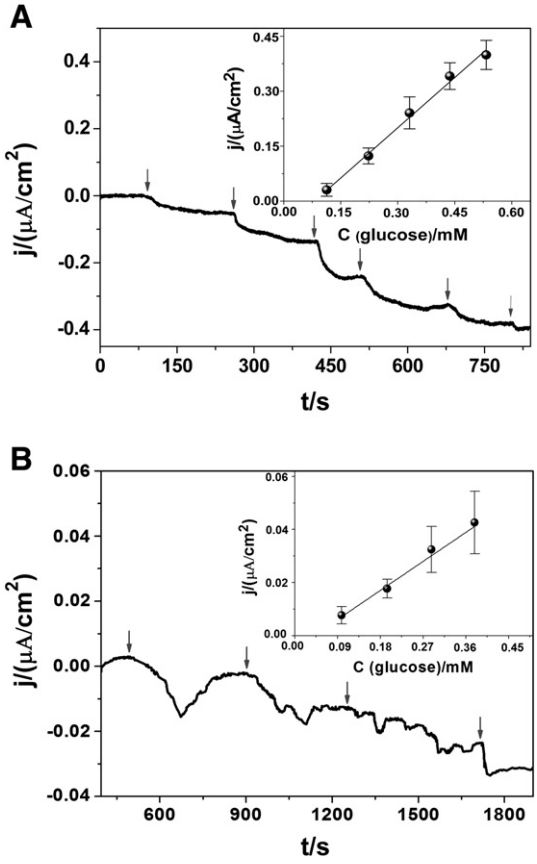

Fig. 5. (A) $(PEI/MP\text{-}11)_2/PEI/(GOx + POPG + DPPG)_1$ and (B) $(PEI/MP\text{-}11)_2/(PEI/GOx)_1$ response to glucose in PBS (10 mM, pH 6.3) at 50 mV (vs SCE). Additions correspond to an increase of 0.113 mM in glucose concentration. Inset: respective linear range analytical curves.

biosensor $(PEI/MP\text{-}11)_2/(PEI/GOx)_1$ in Fig. 5B. These biosensors showed a sensitivity of 0.91 ± 0.09 (μA/cm^2)/mM and 0.12 ± 0.04 (μA/cm^2)/mM, and an LOD of 8.6 ± 1.1 μM and 62 ± 2.0 μM, respectively (inset Fig. 5A and B).

We also investigated the amperometric response of biosensors containing GOx encapsulated using a single phospholipid, as shown in Fig. 6A and B. Biosensors composed of only DPPG showed a sensitivity of 0.45 ± 0.12 (μA/cm^2)/mM and an LOD of 15.2 ± 6.9 μM, whereas units containing POPG encapsulated GOx exhibited a sensitivity of 0.28 ± 0.10 (μA/cm^2)/mM and an LOD of 26.6 ± 7.7 μM. In addition to their lower sensitivities, biosensors containing a single type of phospholipid also showed operational instabilities and low reproducibility. The error bars are indeed very large because the experiments were performed at 37 °C, which is close to the phase transition temperature of DPPG (41 °C). Therefore the use of this lipid does not lead to a good sensor, as expected.

We attribute the effective performance of the biosensor using a 1:4 (v/v) ratio of POPG and DPPG to an improved tuning of the liposome structure due to a balance of the different phase transition temperatures of POPG (−2 °C) and DPPG (41 °C) [36]. Table 1 summarizes the sensitivities and LOD values for all biosensor architectures tested here, while Table 2 shows a comparison between our best architecture and some other glucose biosensors reported in the literature.

The presence of the possible interferents ascorbate, dopamine, paracetamol, lactose, fructose, uric acid and ureate were tested by adding aliquots of these substances intercalated with addition of the analyte solution. This was done by first subjecting the unbiased electrodes (50 mV) to a glucose solution of 10 mM until the current reached a steady-state value. Then, injections were made of 100 μL of each of the interferents. In the presence of ascorbic acid and dopamine the current

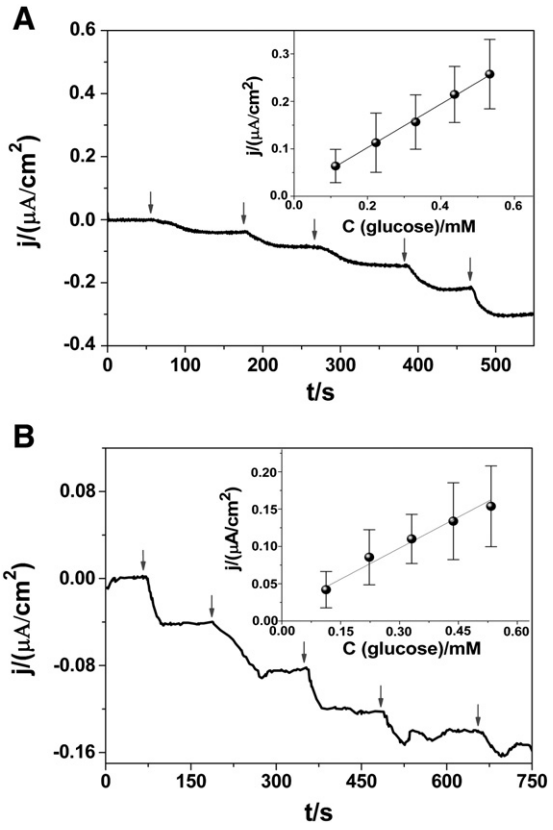

Fig. 6. (A) $(PEI/MP\text{-}11)_2/PEI/(GOx + DPPG)_1$ and (B) $(PEI/MP\text{-}11)_2/PEI/(GOx + POPG)_1$ response to glucose in PBS (10 mM, pH 6.3) at 50 mV (vs SCE). Additions correspond to an increase of 0.113 mM in glucose concentration. Inset: respective linear range analytical curves.

increased, in contrast to the result for glucose. No change in current due to the interferents paracetamol, lactose, fructose and citric acid were observed. For uric acid, on the other hand, there is a small effect with a decrease in current (Fig. 7). Since the biosensor is primarily aimed at being used in food samples (e.g. milk) where there is no uric acid, this interference would not jeopardize the bionsensor's use.

Finally, to demonstrate the biosensor operation in a complex medium, zero-lactose milk samples, known to have a high concentration of glucose (4.5 g in 200 mL of milk, according to the label in the milk package) were used. For the experiments, an aliquot of 2 mL of milk was taken and diluted in PBS up to a concentration of 25 mM of glucose. Thus, aliquots of 20 μL were added to the electrochemical cell (7 mL). Fig. 8 shows the amperometric response of $(PEI/MP\text{-}11)_2/PEI/(GOx + POPG + DPPG)_1$ biosensor for detecting glucose.

The addition of zero-lactose milk produced a reasonable increase in current. The inset shows an average sensitivity of 0.68 ± 0.03 (μA/cm²)/mM (LOD of 32.0 ± 4.3 μM). The glucose concentration obtained from the biosensor response was ca. 40% larger than the value

Table 1
Summary of the sensitivities and LODs obtained for the different studied architectures.

Biosensor architecture	Sensitivity/ ($\mu A \cdot cm^{-2}$/mM)	LOD/mM
$(PEI/MP\text{-}11)_2/(PEI/GOx + POPG + DPPG)_1$	0.91 ± 0.09	8.6 ± 1.1
$(PEI/MP\text{-}11)_2/(PEI/GOX)_1$	0.12 ± 0.04	62.0 ± 2.0
$(PEI/MP\text{-}11)_2/(PEI/GOx + DPPG)_1$	0.45 ± 0.12	15.2 ± 6.9
$(PEI/MP\text{-}11)_2/(PEI/GOx + POPG)_1$	0.28 ± 0.10	26.6 ± 7.7

Table 2
Comparison of developed glucose biosensor with other systems using different electron mediators.

Biosensor	Sensitivity (μA/cm²)/mM	LOD (μM)	Reference
GOD–MWCNT	11.3	30	[37]
$K_3Fe(CN)_6$/GOx/MWCNT	20.6	–	[38]
ITO/PB/GOD-PAH	16	0.20	[17]
GOx/Naf/MnO2/GCE	38.2	25.5	[39]
Au/SAM/GOx/PB	0.05	12.5	[40]
Au/MPS/TH/(SCGNPs/TH)n/GOx/HRP	3.8	0.35	[41]
$(PEI/MP\text{-}11)_2/PEI/(GOx + POPG + DPPG)_1$	0.91	8.6	This paper

quoted in the label. We believe that such difference is due to the presence of additives used for conserving the milk for long periods of time. Additionally, even non-additive substances that might contribute to the amperometric signal are present in milk, as some pharmacological compounds reported by Azzouz et al. [42]. Although we were able to detect glucose in a zero-lactose milk sample, its precise quantification still requires further work, especially to identify the effects from additives.

We checked that the glucose concentration is higher than that stated in the milk packages by measuring the concentration with a colorimetric method (kit from Biotecnica, REF 10.008.00). In this independent method, a concentration about 25% higher than expected was obtained,

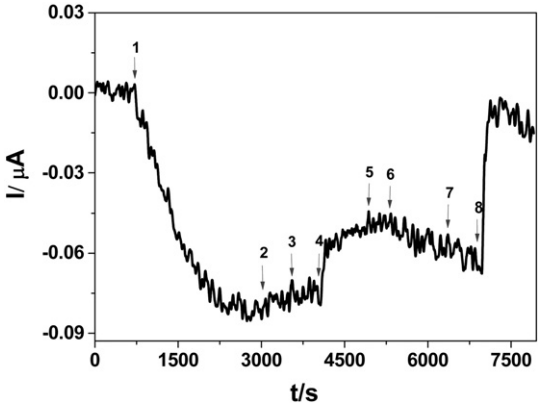

Fig. 7. $(PEI/MP\text{-}11)_2/PEI/(GOx + POPG + DPPG)_1$ response to possible interferents in PBS (10 mM, pH 6.3) at 50 mV (vs SCE). Each addition corresponds to an injection of 100 μL of different substances (1) glucose; (2) fructose; (3) lactose; (4) dopamine; (5) paracetamol; (6) uric acid; (7) citric acid (8) ascorbate at 10 mM.

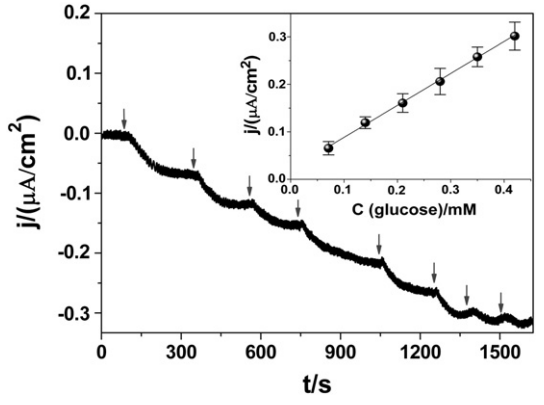

Fig. 8. $(PEI/MP\text{-}11)_2/PEI/(GOx + POPG + DPPG)_1$ response to zero-lactose milk in PBS (10 mM, pH 6.3) at 50 mV (vs SCE). Each addition corresponds to 20 μL of milk (25 mM of glucose). Inset: linear range analytical curve.

consistent with the higher concentration quoted in the present manuscript.

4. Conclusions

In the present work, the combination of LbL and a liposome-encapsulated system was demonstrated to preserve the native structure of biomolecules for an improved biosensor performance. UV–vis spectroscopy measurements revealed a successful growth of PEI/MP-11 and PEI/liposome-encapsulated GOx LbL films. Amperometric results showed that a 2-bilayer PEI/MP-11 LbL film is appropriate for H_2O_2 detection and further use as an electron mediator in a glucose biosensor. The preservation of the native structure of GOX was assessed by circular dichroism spectroscopy, which confirmed the effectiveness of the proposed method. Circular dichroism revealed that 90% of the GOx helical elements are retained during its encapsulation into liposomes and that 60% are retained for liposome-encapsulated GOx assembled as an LbL film. Finally, the biosensor $(PEI/MP\text{-}11)_2/PEI/(GOx + POPG + DPPG)_1$ showed a sensitivity of 0.91 ± 0.09 $(\mu A/cm^2)/mM$, which is 7.5 times that of a similar biosensor fabricated with a non-encapsulated GOx layer (0.12 ± 0.04 $(\mu A/cm^2)/mM$). This improvement in biosensor response was achieved with a specific combination of DPPG and POPG liposomes and we attribute this enhancement to fine tuning of the liposome structure due to their different phase transition temperatures. Finally, the biosensor response toward glucose was also measured in lactose-free milk to demonstrate its efficiency in food samples. Although the detection of glucose could be performed, a precise quantification of it still requires further work, due to the complexity of the sample.

Acknowledgments

This work was supported by FAPESP, CNPq, CAPES and nBioNet network (Brazil).

References

[1] W. Zhao, Y. Fang, Q. Zhu, K. Wang, M. Liu, X. Huang, et al., A novel glucose biosensor based on phosphonic acid–functionalized silica nanoparticles for sensitive detection of glucose in real samples, Electrochim. Acta 89 (2013) 278–283.
[2] A. Sassolas, L.J. Blum, B.D. Leca-Bouvier, Immobilization strategies to develop enzymatic biosensors, Biotechnol. Adv. 30 (2012) 489–511.
[3] N.A. Chaniotakis, Enzyme stabilization strategies based on electrolytes and polyelectrolytes for biosensor applications, Anal. Bioanal. Chem. 378 (2004) 89–95.
[4] G. Ren, H. Yu, Oriented adsorptive immobilization of esterase BioH based on protein structure analysis, Biochem. Eng. J. 53 (2011) 286–291.
[5] S.A. Ansari, Q. Husain, Potential applications of enzymes immobilized on/in nano materials: a review, Biotechnol. Adv. 30 (2012) 512–523.
[6] S.K. Sharma, N. Sehgal, A. Kumar, Biomolecules for development of biosensors and their applications, Curr. Appl. Phys. 3 (2003) 307–316.
[7] C. Marcuello, R. de Miguel, C. Gómez-Moreno, M. Martínez-Júlvez, A. Lostao, An efficient method for enzyme immobilization evidenced by atomic force microscopy, Protein Eng. Des. Sel. 25 (2012) 715–723.
[8] K. Ariga, Q. Ji, J.P. Hill, Enzyme-encapsulated layer-by-layer assemblies: current status and challenges toward ultimate nanodevices, in: F. Caruso (Ed.), Mod. Tech. Nano-Microreactors-React, Springer Berlin Heidelberg, Berlin, Heidelberg, 2010, pp. 51–87.
[9] Y.S. Lee, Self-assembly and nanotechnology: a force balance approach, John Wiley & Sons, Hoboken, N.J., 2008
[10] K. Ariga, M. Onda, Y. Lvov, T. Kunitake, Alternate layer-by-layer assembly of organic dyes and proteins is facilitated by pre-mixing with linear polyions, Chem. Lett. (1997) 25–26.
[11] G. Decher, J.B. Schlenoff, Multilayer Thin Films: Sequential Assembly of Nanocomposite Materials, John Wiley & Sons, 2012.
[12] A.C. Fou, O. Onitsuka, M. Ferreira, M.F. Rubner, B.R. Hsieh, Fabrication and properties of light-emitting diodes based on self-assembled multilayers of poly(phenylene vinylene), J. Appl. Phys. 79 (1996) 7501–7509.
[13] M. Watanabe, Y. Nakamura, T. Shinagawa, S. Watase, T. Tamai, N. Nishioka, et al., Highly c-axis oriented deposition of zinc oxide on an ITO surface modified by layer-by-layer method, Electrochim. Acta 96 (2013) 237–242.
[14] R. Song, J. Yan, S. Xu, Y. Wang, T. Ye, J. Chang, et al., Silver ions/ovalbumin films layer-by-layer self-assembled polyacrylonitrile nanofibrous mats and their antibacterial activity, Colloids Surf. B: Biointerfaces 108 (2013) 322–328.
[15] J. Zhu, L. Xu, J. He, Assembly of graphene nanosheets and SiO2 nanoparticles towards transparent, antireflective, conductive, and superhydrophilic multifunctional hybrid films, Chem. Eur. J. 18 (2012) 16393–16401.
[16] M. Ferreira, Valtencir Zucolotto, M. Ferreira, Osvaldo N. Oliveira Jr., Karen Wohnrath, Layer-by-layer and Langmuir–Blodgett films from nanoparticles and complexes, Encycl. Nanosci. Nanotechnol, 1st ed., American Scientific Publishers, California, 2003, pp. 441–465.
[17] M. Ferreira, P.A. Fiorito, O.N. Oliveira, S.I.C. de Torresi, Enzyme-mediated amperometric biosensors prepared with the layer-by-layer (LbL) adsorption technique, Biosens. Bioelectron. 19 (2004) 1611–1615.
[18] D. Lee, Y. Chander, S.M. Goyal, T. Cui, Carbon nanotube electric immunoassay for the detection of swine influenza virus H1N1, Biosens. Bioelectron. 26 (2011) 3482–3487.
[19] Y. Xiang, H. Zhang, B. Jiang, Y. Chai, R. Yuan, Quantum dot layer-by-layer assemblies as signal amplification labels for ultrasensitive electronic detection of uropathogens, Anal. Chem. 83 (2011) 4302–4306.
[20] L. Petri, M. Ferreira, M.L. Moraes, Toward preserving the structure of the antigenic peptide p17-1 from the HIV-1 p17 protein in nanostructured films, J. Nanosci. Nanotechnol. 11 (2011) 6705–6709.
[21] M.L. Moraes, L.R. Lima, R.R. Silva, M. Cavicchioli, S.J.L. Ribeiro, Immunosensor based on immobilization of antigenic peptide NS5A-1 from HCV and silk fibroin in nanostructured films, Langmuir 29 (2013) 3829–3834.
[22] M. Yoshimoto, M. Sato, N. Yoshimoto, K. Nakao, Liposomal encapsulation of yeast alcohol dehydrogenase with cofactor for stabilization of the enzyme structure and activity, Biotechnol. Prog. 24 (2008) 576–582.
[23] Q. Liu, B.J. Boyd, Liposomes in biosensors, Analyst 138 (2012) 391–409.
[24] V. Razumas, J. Kazlauskaite, T. Ruzgas, J. Kulys, Bioelectrochemistry of microperoxidases, J. Electroanal. Chem. 343 (1992) 159–176.
[25] R.F. de Oliveira, M.L. de Moraes, O.N. Oliveira, M. Ferreira, Exploiting cascade reactions in bienzyme layer-by-layer films, J. Phys. Chem. C 115 (2011) 19136–19140.
[26] M.L. Moraes, P.J. Gomes, P.A. Ribeiro, P. Vieira, A.A. Freitas, R. Köhler, et al., Polymeric scaffolds for enhanced stability of melanin incorporated in liposomes, J. Colloid Interface Sci. 350 (2010) 268–274.
[27] D. de Lima, W. Alves Andrade, Estudo da transferência eletrônica direta em modelo de peroxidase, http://ic.ufabc.edu.br/II_SIC_UFABC/resumos/paper_5_75.pdf. 2013.
[28] T. Lötzbeyer, W. Schuhmann, H.-L. Schmidt, Electron transfer principles in amperometric biosensors: direct electron transfer between enzymes and electrode surface, Sensors Actuators B Chem. 33 (1996) 50–54.
[29] S. Nicolis, L. Casella, R. Roncone, C. Dallacosta, E. Monzani, Heme-peptide complexes as peroxidase models, C.R. Chim. 10 (2007) 380–391.
[30] L. Zhang, M. Li, X. Huang, Y. Feng, C. Liu, W. Xing, et al., Study on mechanism of interaction between Eu3+ and microperoxidase-11, Electrochim. Acta 52 (2006) 1009–1014.
[31] S. Guo, Q. Zhou, T. Lu, X. Ding, X. Huang, Interaction between La3+ and MP-11 in the physiological solution, Electrochim. Acta 52 (2007) 2032–2038.
[32] W. Huang, Z. Zhang, X. Han, J. Tang, Z. Peng, S. Dong, et al., Electrochemistry and spectroscopy study on the interaction of microperoxidase-11 with lipid membrane, Biophys. Chem. 94 (2001) 165–173.
[33] Y. Astuti, E. Topoglidis, J.R. Durrant, Use of microperoxidase-11 to functionalize tin dioxide electrodes for the optical and electrochemical sensing of hydrogen peroxide, Anal. Chim. Acta. 686 (2011) 126–132.
[34] Z. Xu, N. Gao, H. Chen, S. Dong, Biopolymer and carbon nanotubes interface prepared by self-assembly for studying the electrochemistry of microperoxidase-11, Langmuir 21 (2005) 10808–10813.
[35] T.C. Cipriano, P.M. Takahashi, D. de Lima, V.X.O. Jr, J.A. Souza, H. Martinho, et al., Spatial organization of peptide nanotubes for electrochemical devices, J. Mater. Sci. 45 (2010) 5101–5108.
[36] A.C.F. Xavier, M.L. de Moraes, M. Ferreira, Immobilization of aloin encapsulated into liposomes in layer-by-layer films for transdermal drug delivery, Mater. Sci. Eng. C 33 (2013) 1193–1196.
[37] J. Li, Y.-B. Wang, J.-D. Qiu, D. Sun, X.-H. Xia, Biocomposites of covalently linked glucose oxidase on carbon nanotubes for glucose biosensor, Anal. Bioanal. Chem. 383 (2005) 918–922.
[38] Y.-S. Chen, J.-H. Huang, C.-C. Chuang, Glucose biosensor based on multiwalled carbon nanotubes grown directly on Si, Carbon 47 (2009) 3106–3112.
[39] L. Zhang, S. Yuan, L. Yang, Z. Fang, G. Zhao, An enzymatic glucose biosensor based on a glassy carbon electrode modified with manganese dioxide nanowires, Microchim. Acta 180 (2013) 627–633.
[40] H. Wang, H. Ohnuki, H. Endo, M. Izumi, Effects of self-assembled monolayers on amperometric glucose biosensors based on an organic–inorganic hybrid system, Sensors Actuators B Chem. 168 (2012) 249–255.
[41] Y. Sun, Y. Bai, W. Yang, C. Sun, Controlled multilayer films of sulfonate-capped gold nanoparticles/thionine used for construction of a reagentless bienzymatic glucose biosensor, Electrochim. Acta 52 (2007) 7352–7361.
[42] A. Azzouz, B. Jurado-Sánchez, B. Souhail, E. Ballesteros, Simultaneous determination of 20 pharmacologically active substances in cow's milk, goat's milk, and human breast milk by gas chromatography–mass spectrometry, J. Agric. Food Chem. 59 (2011) 5125–5132.